Remote Sensing **2010**, *2*, 611-640; doi:10.3390/rs2030611

OPEN ACCESS

Remote Sensing

ISSN 2072-4292

www.mdpi.com/journal/remotesensing

Article

Effects of Spatial and Spectral Resolutions on Fractal Dimensions in Forested Landscapes

Mohammad Al-Hamdan [1,*] , James Cruise [2] , Douglas Rickman [3] and Dale Quattrochi [3]

[1] Universities Space Research Association at NASA Marshall Space Flight Center, National Space Science and Technology Center, NASA Global Hydrology and Climate Center, Huntsville, AL 35805, USA

[2] Civil and Environmental Engineering Department, University of Alabama in Huntsville, Huntsville, AL 35899, USA; E-Mail: cruise@cee.uah.edu

[3] Earth Science Office at NASA Marshall Space Flight Center, National Space Science and Technology Center, NASA Global Hydrology and Climate Center, Huntsville, AL 35805, USA; E-Mails: douglas.l.rickman@nasa.gov (D.R.); dale.quattrochi@nasa.gov (D.Q.)

* Author to whom correspondence should be addressed; E-Mail: mohammad.alhamdan@nasa.gov; Tel.: +1-256-961-7465; Fax: +1-256-961-7377.

Received: 28 December 2009; in revised form: 20 February 2010 / Accepted: 21 February 2010 / Published: 26 February 2010

Abstract: Recent work has shown that more research is needed in applying fractal analysis to multi-resolution remote sensing data for landscape characterization. The purpose of this study was to closely examine the impacts that spatial and spectral resolutions have on fractal dimensions using real-world multi-resolution remotely sensed data as opposed to the more conventional single resolution and aggregation approach. The study focused on fractal analysis of forested landscapes in the southeastern United States and Central America. Initially, the effects of spatial resolution on the computed fractal dimensions were examined using data from three instruments with different spatial resolutions. Based on the criteria of mean value and variation within the accepted ranges of fractal dimensions, it was determined that 30-m Landsat TM data were best able to capture the complexity of a forested landscape in Central America compared to 4-m IKONOS data and 250-m MODIS data. Also, among the spectral bands of Landsat TM images of four national forests in the southeastern United States, tests showed that the spatial indices of fractal dimensions are much more distinguishable in the visible bands than they are in the near-mid infrared bands. Thus, based solely on the fractal analysis, the fractal dimensions could have relatively higher chances to distinguish forest characteristics (e.g., stand sizes and species) in the

Landsat TM visible wavelength bands than in the near-mid infrared bands. This study has focused on a relative comparison between visible and near-mid infrared wavelength bands; however it will be important to study in the future the effect of a combination of those bands such as the Normalized Difference Vegetation Index (NDVI) on fractal dimensions of forested landscapes.

Keywords: remote sensing; fractal dimensions; spatial and spectral resolutions; forested landscapes

1. Introduction

Essential issues in interpretation and analysis of remotely sensed data are the resolution and scale of the observations [1]. Scale is crucial to the characterization of geospatial data because many environmental processes are scale-dependent [2]. One of the principal methods that can be used to examine scale effects is through the use of fractal analysis. Fractals are based on the concept of self-similarity in the geometry of natural objects. Fractal analysis has been used to analyze the scale dependence of everything from topographic surfaces [3] to microstructures [4] to the structure of rainstorms [5].

One area where fractal analysis has recently been found useful is in characterization of surfaces using remotely sensed data [1,6-9]. However, problems arise because the computed fractal dimensions will be affected by the spatial scale of the remotely sensed data as well as the spectral characteristics of the instrument and the bands in which the data are recorded. This has made it difficult to compare results across studies that used different instruments. Quattrochi *et al.* [1], Emerson *et al.* [6], and Lam *et al.* [7] concluded in their studies that more research is needed in applying fractal analysis to multi-resolution remote sensing data for landscape characterization. The purpose of this study was to closely examine the impacts that spatial and spectral resolutions have on fractal dimensions using real-world multi-resolution remotely sensed data as opposed to the more conventional single resolution and aggregation approach or simulated surfaces. Those impacts were studied in terms of the ability of fractal dimensions to capture the complexity of forested landscapes at different spatial and spectral resolutions. The study focused on fractal analysis of forested landscapes in the southeastern United States and Central America.

2. Fractals

Spatial patterns in nature are irregular and fragmented [7] such that they cannot be adequately described by classical Euclidian geometry. Fractal geometry was developed as a means of characterizing such complex natural patterns [10]. The foundation for fractal analysis is self-similarity [7,10]. Self-similarity can be defined as a property of a curve or surface where each part is indistinguishable from the whole [1,7]. Many curves and surfaces are statistically "self-similar," meaning that each portion can be considered as a reduced-scale image of the whole [1]. In classical geometry, a point has an integer topological dimension of zero, a line has one dimension, an area has

two dimensions, and a volume has three dimensions [1,7]. The fractal dimension (FD), however, is a non-integer value that exceeds the Euclidean topological dimension [7,10]. The fractal dimension increases as the form of a point pattern, a line, or an area feature grows more geometrically complex [7]. The fractal dimension of a point pattern can vary between zero and one, that of a curve can vary between one and two, and that of a surface can vary between two and three [1,7]. FD values approach 3.0 as the geometrical complexity of a perfectly flat two-dimensional surface (FD = 2.0) increases so that the surface begins to fill a volume [7].

For a surface, such as raster-based remotely sensed images, FD can be estimated using the isarithm method which was evolved from Goodchild [11], Shelberg *et al.* [12], and Lam and DeCola [13]. Lam *et al.* [14] found that the isarithm method calculates the FD fairly accurately and more so than other methods such as the variogram and triangular prism methods. The isarithm method, sometimes also called the walking-divider method utilizes the isarithms of the surface as a means in determining the FD of the surface [14]. As a flat surface grows more complex, FD increases from a value of 2.0 and approaches 3.0 as the surface begins to fill a volume. The final fractal dimension FD of the surface is the average of the FD values for those isarithms having a coefficient of determination "R^2" greater than or equal to 0.9 [1,7,8,15].

Fractal analysis yield quantitative values on the spatial complexity and information content contained within multi-scale remote sensing data because of self-similarity [1]. Thus, different spatial, temporal and spectral resolutions remote sensing data acquired from different sensors could be compared and evaluated based on fractal measurements. Moreover, a quantitative description of surface roughness or complexity may aid mapping and interpretation of landscapes or characterization of resources such as forest density or biomass.

As discussed previously, fractals can be applied to a variety of landscape problems because they conveniently describe many irregular, fragmented patterns found in nature [10]. Although the fractal technique and other textural analyses have been applied extensively [5,16-28], its use as a spatial technique for characterizing remote sensing images needs to be evaluated more thoroughly in terms of the affects of spatial and spectral resolution [1,6,7]. This study deals with the utility of fractals to characterize the complexity of forest surfaces or canopies at different spatial and spectral resolutions.

This effect is demonstrated in Figure 1, which illustrates that for a given pixel resolution, as the crown width decreases, the image complexity decreases. The values of the adjacent pixels become more similar because the pixel values are the integration of the brightness levels within that pixel. The image is represented and displayed in a digital format by subdividing the image into small equal-sized and shaped areas, called picture elements or pixels, and representing the brightness of each area with a numeric value or digital number which is the integration of the brightness levels within that pixel.

If the two adjacent pixels are covered with small crown trees as in Figure 1(a), the result is two homogenous surfaces, and so the integration result of both pixels will be close, and thus the two pixel values will be similar in magnitude. If the pixel values do not vary significantly, the result is less complexity in terms of fractals and more homogeneity in terms of autocorrelation and so smaller Fractal Dimensions.

On the other hand, if the pixels are covered with large crown trees as in Figure 1(b), the result is non-homogenous adjacent pixels, and so the integration result in both pixels will not be similar, and thus the two pixel values will not be close in magnitude. If the pixel values vary significantly, this

means more complexity in terms of fractals, less homogeneity in terms of autocorrelation, and results in higher Fractal Dimension.

Figure 1. Size class effect on remotely sensed data: **(a)** small crown trees **(b)** large crown trees.

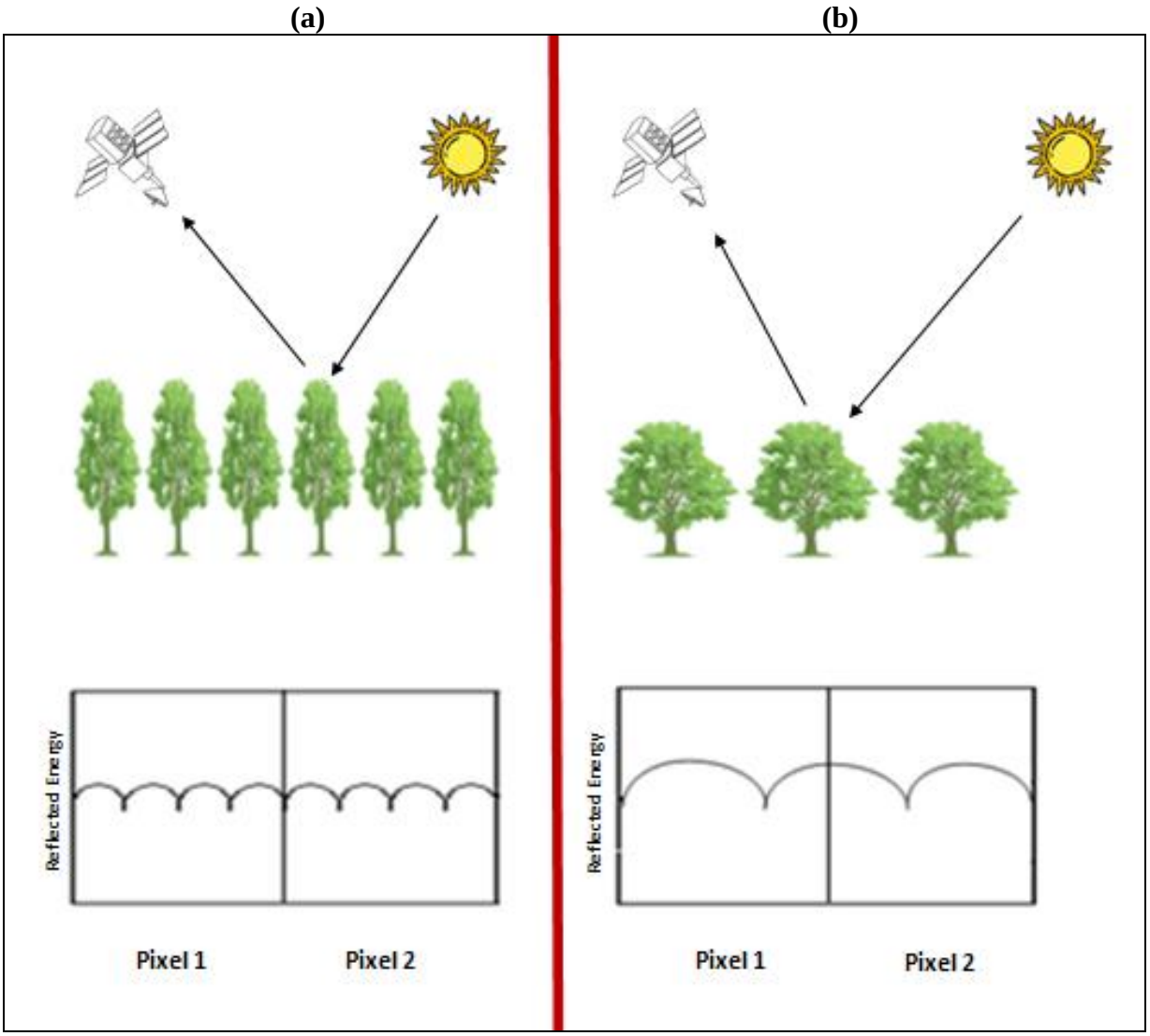

3. Spatial Resolution Effects

The first phase of the study was to determine the effect of spatial resolution of the remotely sensed data (*i.e.*, measurement scale) on the estimates of the fractal dimensions used to determine surface roughness and complexity associated with forests. In order to address this issue, several remote sensing images of different spatial resolution (*i.e.*, multiscale remotely sensed data) were obtained for the same forested location. Fractals were used to characterize these images in terms of image complexity and roughness associated with forests.

An important role in employment of remotely sensed imagery has been scale variation and sensitivity [29-31]. The problem of selecting appropriate resolutions is complex [32]. The appropriate resolution is a function of the kind of information desired, the type of environment, and the techniques used to extract information. In order to capture the change in image characteristics due to changes in

resolution, and find relationships between accuracy and resolutions, it is necessary to build a framework to represent, analyze and classify images from multiple resolutions [32]. This framework could be a useful tool for selecting the appropriate spatial resolutions and analysis routines in further image classification [31,33-35].

Many studies reported in the literature have used multiple resolution remote sensing data to study changes in vegetation indices [30,36], surface complexity and variation [1,7-9,37], classification accuracy and errors [34,35,38], image representation and storage [31], and ecosystem and landscape analysis in general [39,40]. However, much of the previous research has been devoted to exploring the magnitude and impact of scale or resolution effects by aggregation of a single data set (*i.e.*, re-sampling the data) [32]. Quattrochi *et al.* [1], Emerson *et al.* (6) and Lam *et al.* [7] concluded that more research is needed in applying fractal analysis to multi-resolution remote sensing data for landscape characterization. This work focuses on a real-world multi-resolution fractal analysis of remotely sensed data by analyzing images of the same location at several resolution levels as opposed to the more conventional single resolution and aggregation approach.

3.1. Study Area and Data Sets

In order to study the effect of scale or spatial resolution on fractal dimensions, several remote sensing images of different spatial resolution (*i.e.*, multiscale remotely sensed data) were obtained for the same forested area. The study site is the Maya Biosphere Reserve of Guatemala's department of the Petén that is located in northern part of the Central American country of Guatemala. The selection of this site was based on the availability of several spatial resolution data sets for it at NASA's National Space Science and Technology Center in Huntsville, Alabama.

Spanning approximately 2 million hectares of northern Guatemala, the Maya Biosphere Reserve (MBR) is an area of lowland tropical forests and expansive freshwater wetlands, part of the largest contiguous tropical moist forest remaining in Central America [41]. In general, the forests can be divided into 11 types, according to rainfall and elevation. Guatemala has more than 300 broad-leafed tree species, with the main commercial species being *Dialum spp.* and *Brosium spp*. Coniferous forests are particularly prevalent above elevation 1,200 meters and are the dominant forest type outside El Petén. Pines (especially *Pinus oocarpa*, *P. psuedostrobus* and *P. tenuifolia*) are the most common coniferous species. Montane coniferous forests are often mixed with *Quercus spp*. and *Cupressus lusitanica*. Mangrove forests occur on both the Caribbean and Pacific coasts.

The MBR is a complex of delineated management units including five national parks, four biological reserves (*biotopos*), a multiple use zone, and a buffer zone. The training site of this study is 11 km by 11 km within the national parks of this reserve (see Figure 2). Three different remotely sensed data sets with different spatial resolutions were available for this site (250 m, 30 m, and 4 m) captured by three different sensors mounted on three different satellites. The instruments are Moderate Resolution Imaging Spectroradiometer (MODIS), Thematic Mapper (TM), and Space Imaging (IKONOS), respectively.

The Moderate Resolution Imaging Spectroradiometer (MODIS) is one of a number of instruments carried on board the Terra platform, which was launched in December 1999. MODIS provides continuous global coverage every one to two days, and collects data from 36 spectral bands. Two

bands (1–2) have a resolution of 250 meters. Three bands (3–5) have a resolution of 500 meters. The remaining bands (6–36) have a resolution of 1,000 meters. Band designations of MODIS are shown in Table 1. Figure 3 shows the MODIS multiple spectral images of the study area. These data were obtained from the NASA Land Processes Distributed Active Archive Center (LP DAAC). Bands 1 through 7 were the only available data. Bands 6 and 7 were not utilized in the study.

Figure 2. Guatemala study area location.

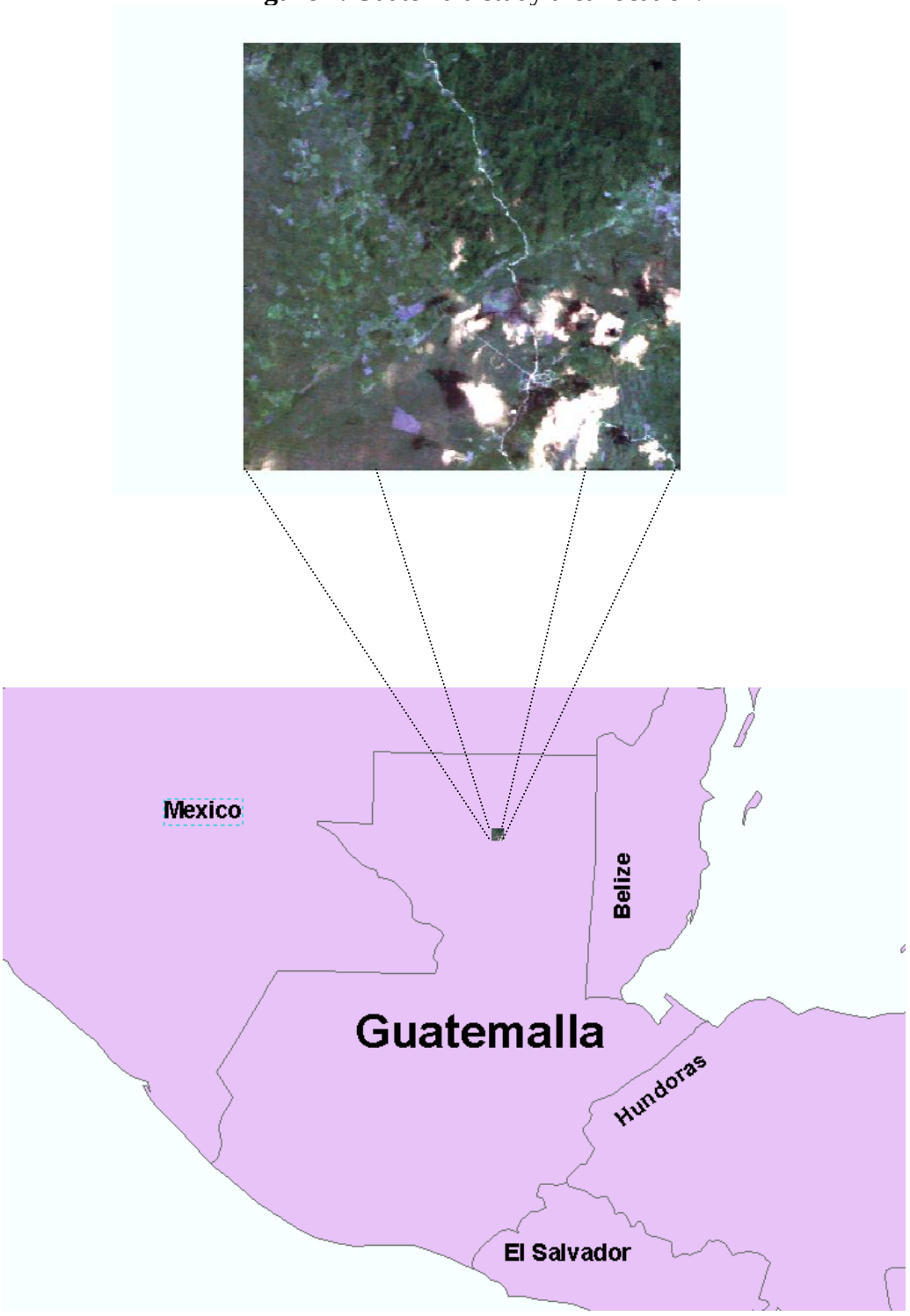

Table 1. MODIS band designations.

BAND	Wavelength (micrometers)	Resolution (meters)
1	0.620–0.670	250
2	0.841–0.876	250
3	0.459–0.479	500
4	0.545–0.565	500
5	0.1230–0.1250	500
6	0.1628–0.1652	1,000
7	2.105–2.155	1,000
8	0.405–0.420	1,000
9	0.438–0.448	1,000
10	0.483–0.493	1,000
11	0.526–0.536	1,000
12	0.546–0.556	1,000
13h	0.662–0.672	1,000
13l	0.662–0.672	1,000
14h	0.673–0.683	1,000
14l	0.673–0.683	1,000
15	0.743–0.753	1,000
16	0.862–0.877	1,000
17	0.890–0.920	1,000
18	0.931–0.941	1,000
19	0.915–0.965	1,000
20	3.660–3.840	1,000
21	3.929–3.989	1,000
22	3.929–3.989	1,000
23	4.020–4.080	1,000
24	4.433–4.498	1,000
25	4.482–4.549	1,000
26	1.360–1.390	1,000
27	6.535–6.895	1,000
28	7.175–7.475	1,000
29	8.400–8.700	1,000
30	9.580–9.880	1,000
31	10.780–11.280	1,000
32	11.770–12.270	1,000
33	13.185–13.485	1,000
34	13.485–13.785	1,000
35	13.785–14.085	1,000
36	14.085–14.385	1,000

Figure 3. Multiple spectral images of MODIS data for Guatemala study area.

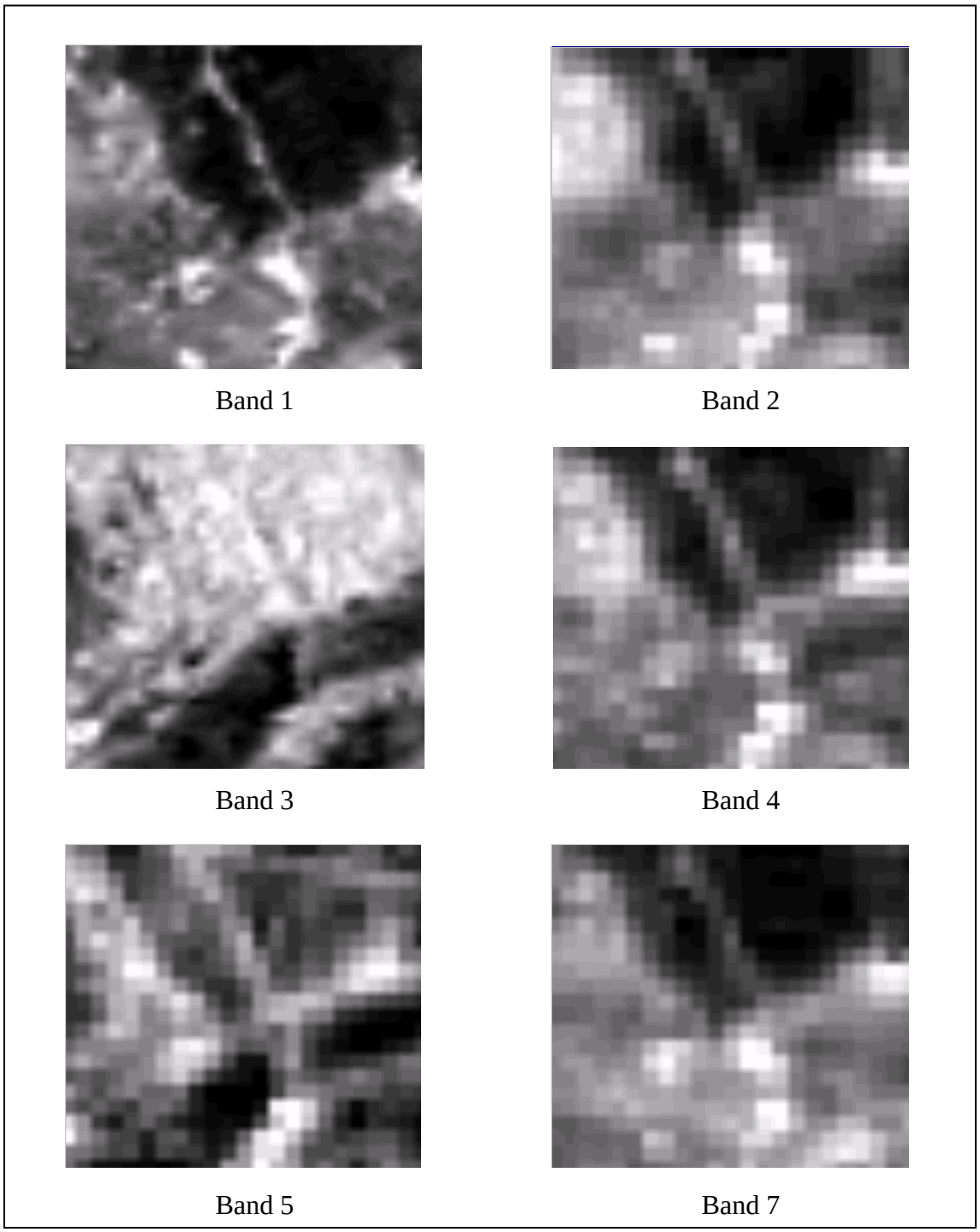

Thematic Mapper (TM) is a multispectral scanning radiometer that is carried on board the Landsat platforms. The TM sensors have provided nearly continuous coverage from July 1982 to present, with a 16-day repeat cycle. TM image data consists of seven spectral bands with a spatial resolution of 30 meters for most bands (1–5 and 7). Resolution for the thermal infrared (band 6) is 120 meters. Band designations are shown in Table 2. Figure 4 shows the Landsat TM multiple spectral images of the study area. The approximate scene size is 11 × 11 kilometers which incorporates 367 × 367 pixels. These data were obtained from the EROS Data Center of the United States Geological Survey (USGS). Those Landsat TM scenes were originally processed with the Standard Terrain Correction (Level 1T)

which provides systematic radiometric and geometric accuracy by incorporating ground control points while employing a Digital Elevation Model (DEM) for topographic accuracy.

Figure 4. Multiple spectral images of Landsat TM data for Guatemala study area.

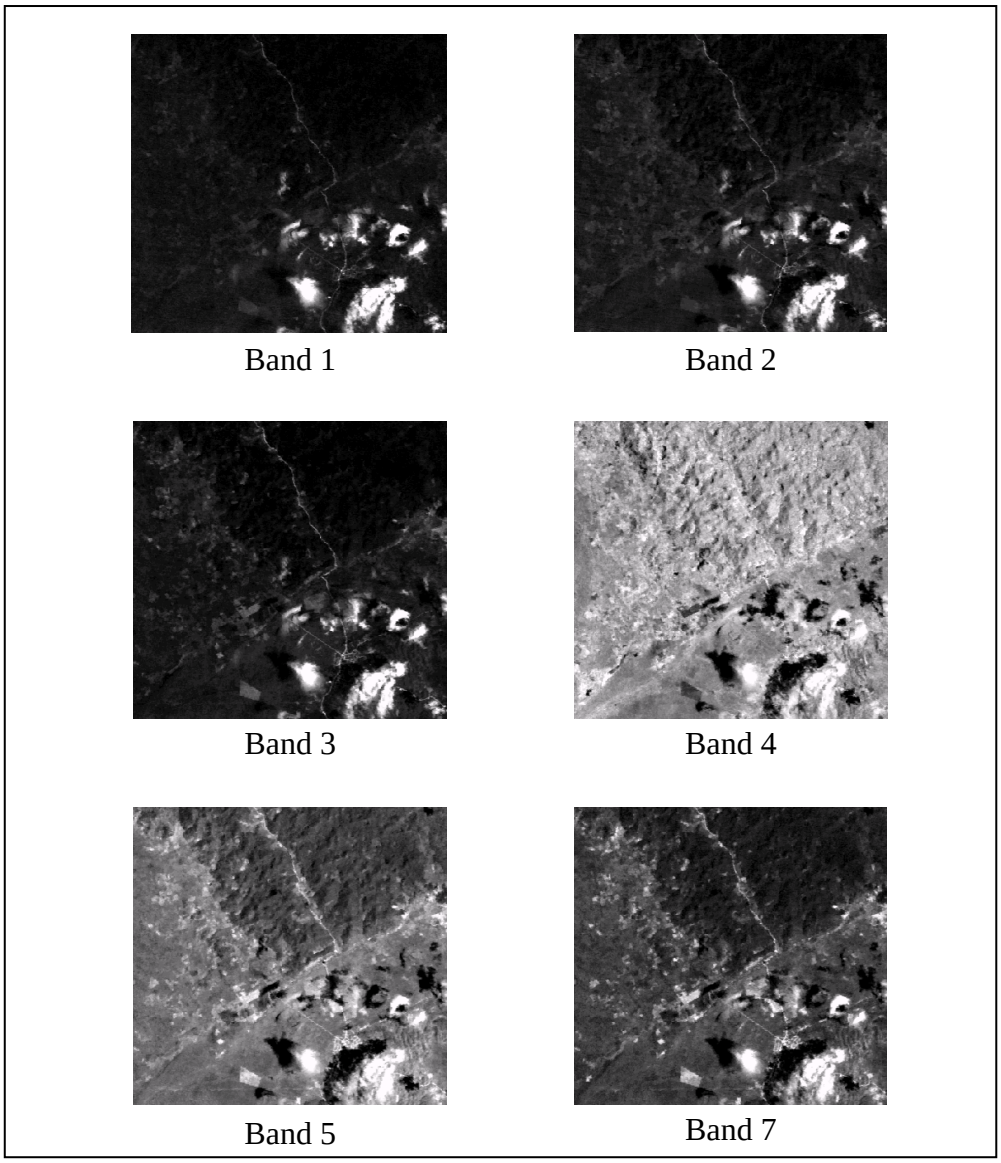

Space Imaging's IKONOS imagery data consists of four spectral bands with a spatial resolution of 4 meters for all bands. Band designations are shown in Table 3. Figure 5 shows the IKONOS multiple spectral images of the study area. The scene size is 11 × 11 kilometers which incorporates 2,750 × 2,750 pixels. These data were obtained from NASA's Scientific Data Purchase Program.

Previous work employing spatial statistical techniques, particularly fractal analysis of remote sensing data, have found that the influence of atmospheric effects on the overall statistical analysis results is very little [1,6,9], thus atmospheric correction of the satellite data for the analysis of this study was not deemed necessary.

A visual study of the Figures 3 through 5 can show that the images of IKINOS which have the finest spatial resolution are the clearest images, followed by Landsat TM images, while the images of MODIS which have the coarsest spatial resolution were the least clear images. This is due to the fact

that the finer the resolution, the more pixels the satellite image which covers a certain area will have, and the more details the satellite image will pick up.

Table 2. Thematic Mapper (TM) band designations.

Band	Wavelength (micrometers)	Resolution (meters)
Band 1	0.45–0.52	30
Band 2	0.52–0.60	30
Band 3	0.63–0.69	30
Band 4	0.76–0.90	30
Band 5	1.55–1.75	30
Band 6	10.40–12.50	120
Band 7	2.08–2.35	30

Table 3. IKONOS band designations.

Band	Wavelength (micrometers)	Resolution (meters)
Band 1	0.445–0.516	4
Band 2	0.506–0.595	4
Band 3	0.632–0.698	4
Band 4	0.757–0.853	4

Figure 5. Multiple spectral images of IKONOS data for Guatemala study area.

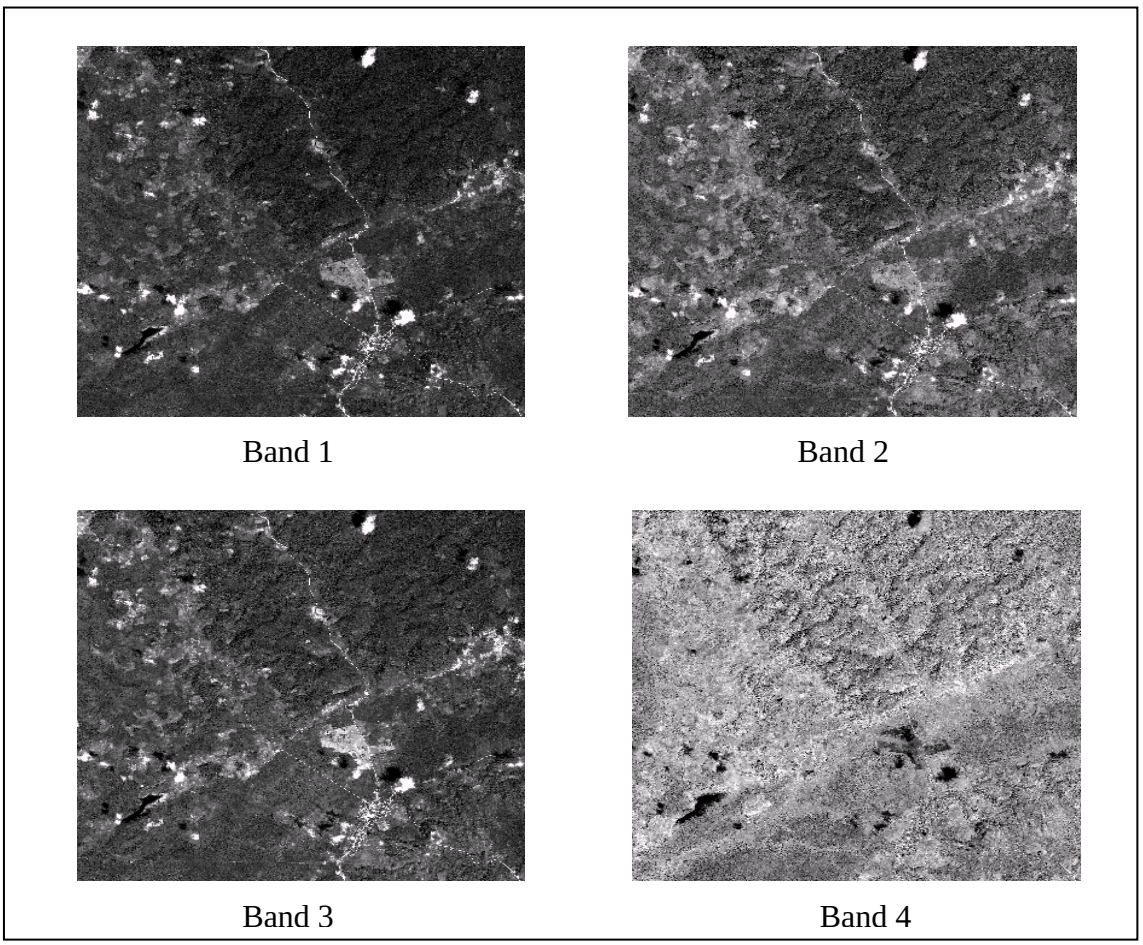

3.2. Methodology

Only the images of similar wavelength channels among the three different resolution data sets should be used in order to focus on studying the effect of spatial resolution alone without any interference by the effect of spectral characteristics. After comparing the ranges of wavelengths of the bands in all data sets, it turned out that the visible bands were the ones that the three different spatial resolution data sets had most in common. The visible bands 1, 3, and 3 of MODIS, Landsat TM, and IKONOS respectively have the most similar wavelengths and were used in the analysis of this study. The GIS module ICAMS [9,37] was used to perform the fractal analysis of the remotely sensed data. ICAMS provides the ability to calculate fractal dimensions of remotely sensed images using the isarithm, variogram [3] and triangular prism methods [42]. The advanced geographic image processing software ER Mapper 6.2 was used to display and enhance raster data. The GIS software, ARCINFO 8.2, was used to overlay vector and raster data as well as link data from geographic and land information systems. The isarithm method was employed within the ICAMS software to compute the fractal dimensions of the image samples.

Thirty samples were collected randomly from each image making sure to obtain equal coverage of all parts of the forest. Criteria for the selection of sample size were based on the resolution, minimum mapping unit size, and nature of the classes to be identified [43]. A smaller window size does not necessarily convey sufficient spatial or texture information to characterize land use types. On the other hand, if the window size is too large, too much information from other land use types could be included and hence the algorithm might not be efficient. Myint [43] and Zhao [44] used sample sizes from 30 × 30 pixels to 120 × 120 pixels for Landsat TM data. Since this study area is only 11 kilometers square and in order to collect as many samples as possible, the sample size for Landsat TM images was chosen to be 1 kilometer square. The selected sample size covers 32 × 32 pixels. In order to cover the same area and location of each sample in MODIS and IKONOS images, the window sizes of each sample were 4 × 4 pixels and 250 × 250 pixels, respectively. Table 4 shows the results of the fractal calculations for all three instruments and Figure 6 shows the FD plots. The table and figure show the FD for the single visible bands used in the analysis for each instrument.

3.3. Results and Discussion

A one-way ANOVA test was conducted using the means of the fractal dimensions among the three different spatial resolution data sets (4 meters, 30 meters, and 250 meters). The mean FD and standard deviation of the data are given at the bottom of the data columns for each instrument on Table 4. The ANOVA test showed that the three means are significantly different at the 0.05 significance level (p value < 0.001) in fractal dimensions (FD). The significance level was chosen to be 0.05 based on the research literature in the areas of remote sensing at different scales and land characterization [8,45-47]. As shown in Table 4 and Figure 6, the finest resolution data (*i.e.*, 4 meters) had the highest fractal dimensions among samples (average FD = 2.95), followed by the 30-meter spatial resolution data (average FD = 2.78), and the most coarse spatial resolution data (*i.e.*, 250 meters) had the lowest fractal dimensions (average FD = 2.47).

Even aside from the statistical significance, these differences can be considered large. For instance, even in the case of different land covers (*i.e.*, urban, forest, or agricultural), investigators have found

that the differences in FD are of the same magnitude as given above. For example, Zhao [44] found, using Landsat TM data (30-meter resolution), that the average FD for an urban study area was 2.69, the average FD for a forest study area was 2.81, the average FD for an agricultural study area was 2.62, and the average FD for a coastal study area was 2.73. In another study, Emerson *et al.* [8] found, using ATLAS data (10-meter resolution), that the average FD for an urban study area was 2.74, the average FD for a forest study area was 2.86, and the average FD for an agricultural study area was 2.61, and the average FD for a coastal study area was 2.73.

Table 4. Fractal dimension results of Guatemala study area for different resolution data.

	IKONOS (4-m resolution)	Landsat TM (30-m resolution)	MODIS (250-m resolution)
1	2.9385	2.7401	2.4482
2	2.9808	2.7295	2.3846
3	2.9310	2.7488	2.5721
4	2.9682	2.8996	2.5277
5	2.9760	2.8290	2.2712
6	2.8102	2.7972	2.4103
7	2.9828	2.8138	2.6507
8	2.8734	2.8304	2.5402
9	2.9661	2.8416	2.3777
10	2.9800	2.8772	2.6066
11	2.9589	2.7318	2.4584
12	2.9412	2.8161	2.4855
13	2.9774	2.9283	2.4857
14	2.9786	2.7356	2.5165
15	2.9356	2.6980	2.4528
16	2.9529	2.7347	2.5698
17	2.9590	2.7467	2.6343
18	2.9793	2.7262	2.5749
19	2.9718	2.7110	2.3860
20	2.9815	2.8275	2.4622
21	2.8933	2.7747	2.3647
22	2.9765	2.6507	2.4330
23	2.9292	2.7990	2.3608
24	2.9646	2.7842	2.4082
25	2.9373	2.8063	2.4375
26	2.9250	2.7210	2.5292
27	2.9054	2.8278	2.4564
28	2.9512	2.7569	2.5435
29	2.9300	2.7139	2.5190
30	2.9259	2.6807	2.3747
Average:	**2.9461**	**2.7759**	**2.4747**
Std. Dev.:	**0.0382**	**0.0655**	**0.0903**

Figure 6. Fractal dimension results of Guatemala study area for different spatial resolution data sets.

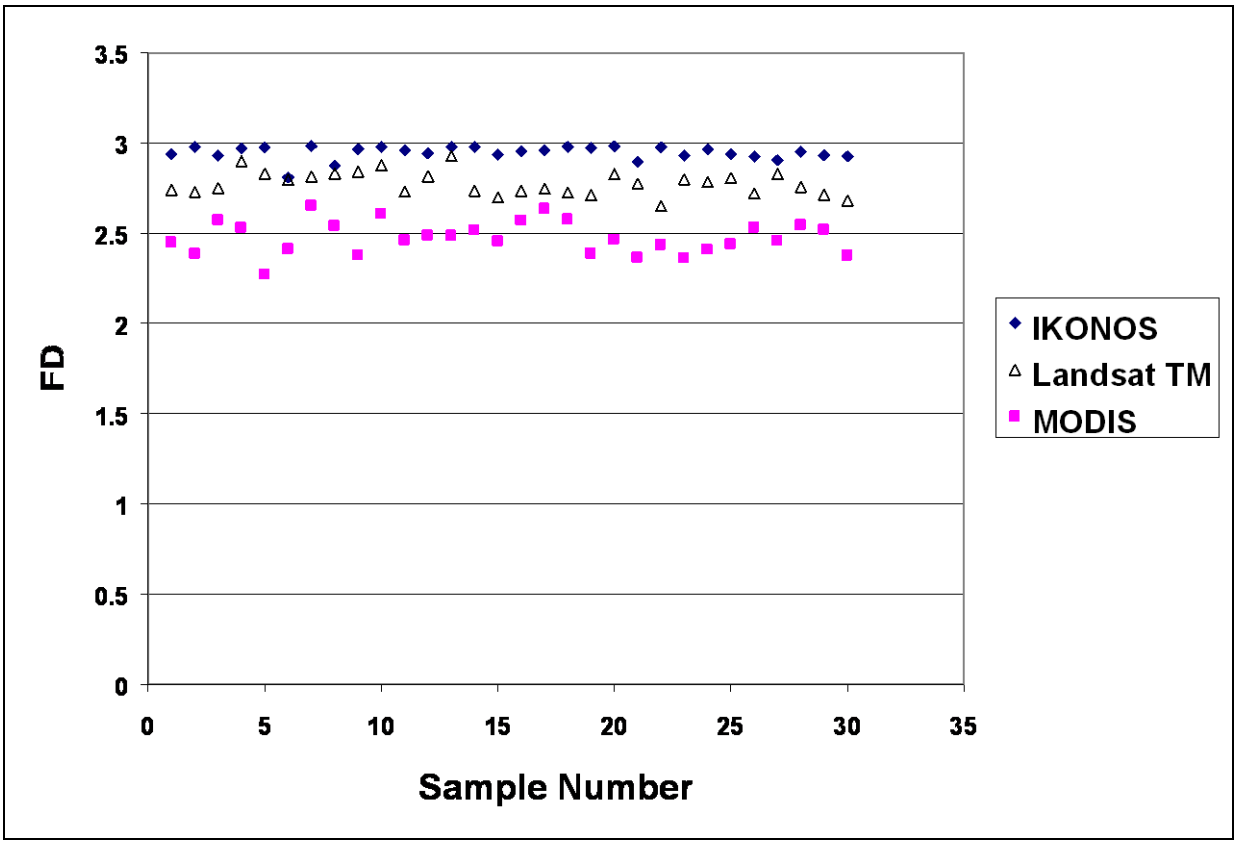

The results of this study (*i.e.*, the fractal dimension was the highest for the finest spatial resolution (4 meters) and the lowest for the coarsest spatial resolution (250 meters)) are due to the fact that the finer the resolution, the more details the satellite image will pick up within an area, and so the more complex it will become. These results agree with the results of Emerson *et al.* [8] who found that larger pixel size in the forested scene decreases the complexity of the image as individual clumps of trees are assimilated into larger blocks. Emerson *et al.* [8] also concluded that it is likely that the tortuosity of isarithms of gray values in the forested image, as indicated by a higher FD value, would be greater if the sensor were able to resolve individual trees within the scene. That is why the 4-m resolution IKONOS data had much higher fractal dimensions than the 30-m resolution Landsat and the 250-m resolution MODIS data sets in this study.

A Bartlett's χ^2 test [48] on the variances of the three data sets revealed that they are also different at the 0.05 significance level (B > 5.991). Comparisons of the results show that the 4-meter resolution IKONOS data have the lowest variation in the fractal dimensions (standard deviation = 0.0382) followed by the TM (s.d. = 0.0655) and then the MODIS (s.d. = 0.0903). In interpreting these results, it is convenient to make use of previous research on fractal analysis from remote sensing data. It has been demonstrated by numerous investigators [1,6,7,9] that fractal dimensions derived from remotely sensed data fall within a practical range of 2.5 to 3.0, with a value of 2.5 effectively representing a water body and 3.0 corresponding to a three dimensional image. Thus, for the FD to effectively capture the variation in surface complexity of a remotely sensed image, one would like for the computed sample values to freely range within those bounds. Now, in the case of the 4-m resolution

IKONOS data, the fine spatial resolution revealed so much detail on the image that the fractal dimension remained near the upper bound (range = 2.81–2.98). On the other hand, although the 250-meter resolution image resulted in the highest variation in the fractal dimensions (standard deviation = 0.0903), the relative lack of detail in those images resulted in FD values that fell below the optimum range (range = 2.27–2.65). Based on results gained from previous experience, it would be very difficult to interpret values in that range, particularly those below 2.5. However, the 30-meter resolution image evidenced a variation in the fractal dimensions that fell fairly in the accepted range (range = 2.65–2.928). In other words, the Landsat TM images resulted in FD values that would ultimately be of more practical use than MODIS and more sensitive to changes in landscape complexity than IKONOS. Thus, the conclusion is that Landsat TM 30-meter resolution data would be better than IKONOS 4-meter and MODIS 250-meter data for the purpose of detecting potential differences in forest characteristics using fractal dimensions.

4. Spectral Characteristics Effect on Spatial Indices

The results of the previous section appear to indicate that, among the spatial resolutions tested, the 30-m TM data were best suited for evaluation of forested landscapes using fractal dimensions. It should be remembered that the FD results analyzed in the previous section were average values computed from particular visible bands of the three instruments. The next question to be answered then is, among the spectral bands available on the TM instrument, which are most suitable for fractal analysis? This section is designed to illustrate the effect of spectral characteristics of the different TM bands on fractal measurements in forested landscapes. However, this time four different Landsat TM images were obtained for four forested areas in the southeastern United States. The forests analyzed were the Talladega, Oakmulgee, and Bankhead National Forests in Alabama, and the Chattahoochee National Forest in Georgia (Figure 7). The forests are operated by the U.S. National Forest Service and encompass areas of 61,904 ha, 128,638 ha, 148,475 ha, and 26,209 ha respectively. The forests contain a mixture of softwood and hardwood species with softwoods (longleaf slash pine, shortleaf loblolly, cypress) predominating by about 58.5% to 41.5% in all of the forests except Talladega where the hardwoods (white oak, hickory, ash, yellow poplar) barely predominate (52% to 48%). Elevations vary among the areas from a low of 60–170 m above mean sea level in the Oakmulgee forest to a high of 210–538 m above mean sea level in the Talladega forest. Landsat TM images of these forests were obtained representing the Summer 2000 period for the Talladega and Chattahoochee forests and for the Summer 1999 window for the Oakmulgee and Bankhead forests. Figures 8–11 show images of the visible and infrared TM bands for all study areas.

The data were processed in much the same way as described in the case of the spatial resolution analysis. After initial processing, samples were randomly selected from the image for each forest, again making sure to cover the entire forest each time. The selected sample size was 100 × 100 pixels based on reported literature [43,44]. The total numbers of collected samples were 36, 52, 32, and 31 for the Talladega, Oakmulgee, Bankhead, and Chattahoochee National Forests respectively. The raster data of the samples were then imported into ICAMS where the fractal dimensions were computed for each band. The FD results are plotted in Figures 12–15. The descriptive statistics of the FD values for all bands are given in Tables 5–8 for each study area.

Figure 7. Location of Bankhead, Oakmulgee, Talladega, and Chattahoochee National Forests.

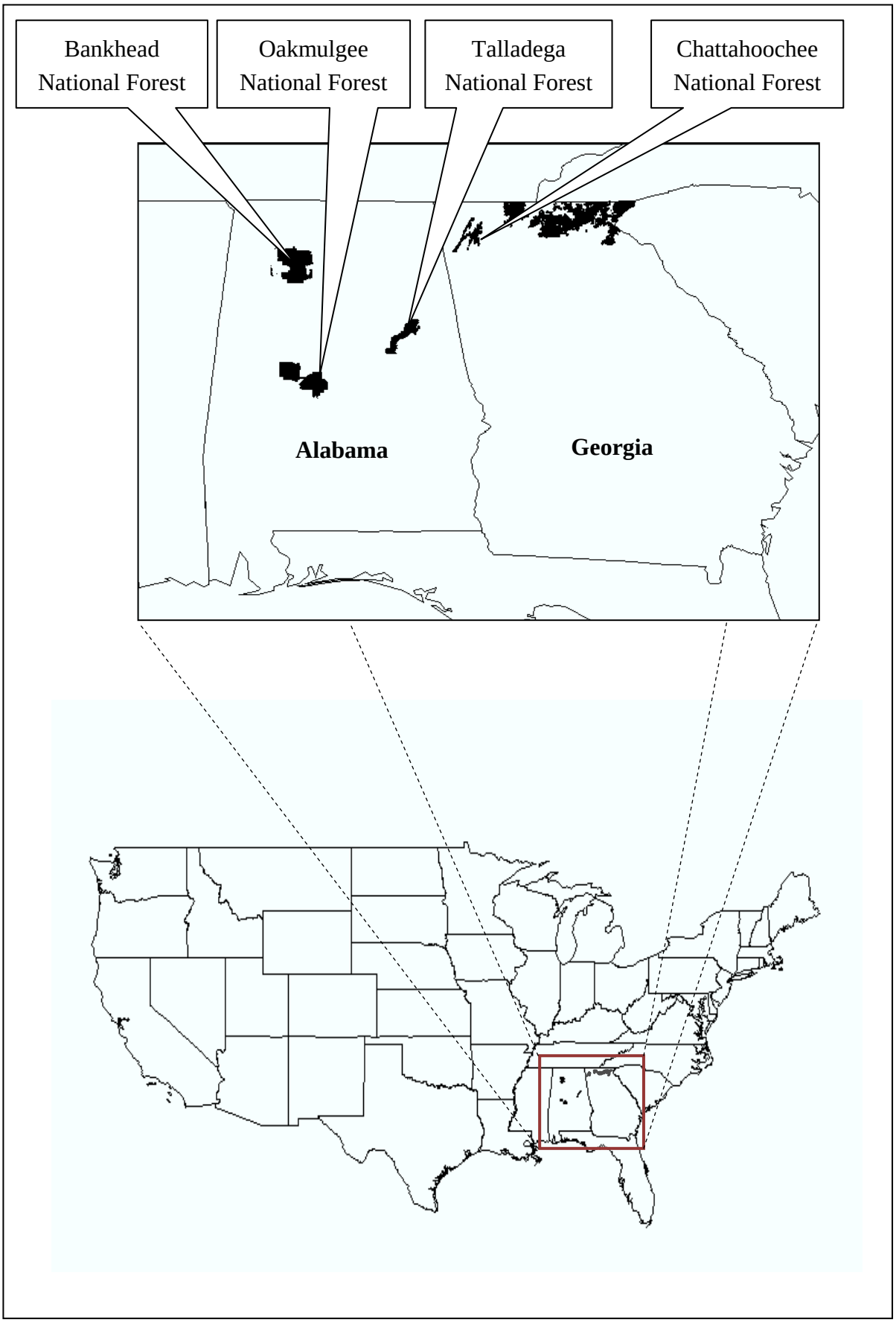

Figure 8. Multiple spectral images of Talladega National Forest, AL, USA.

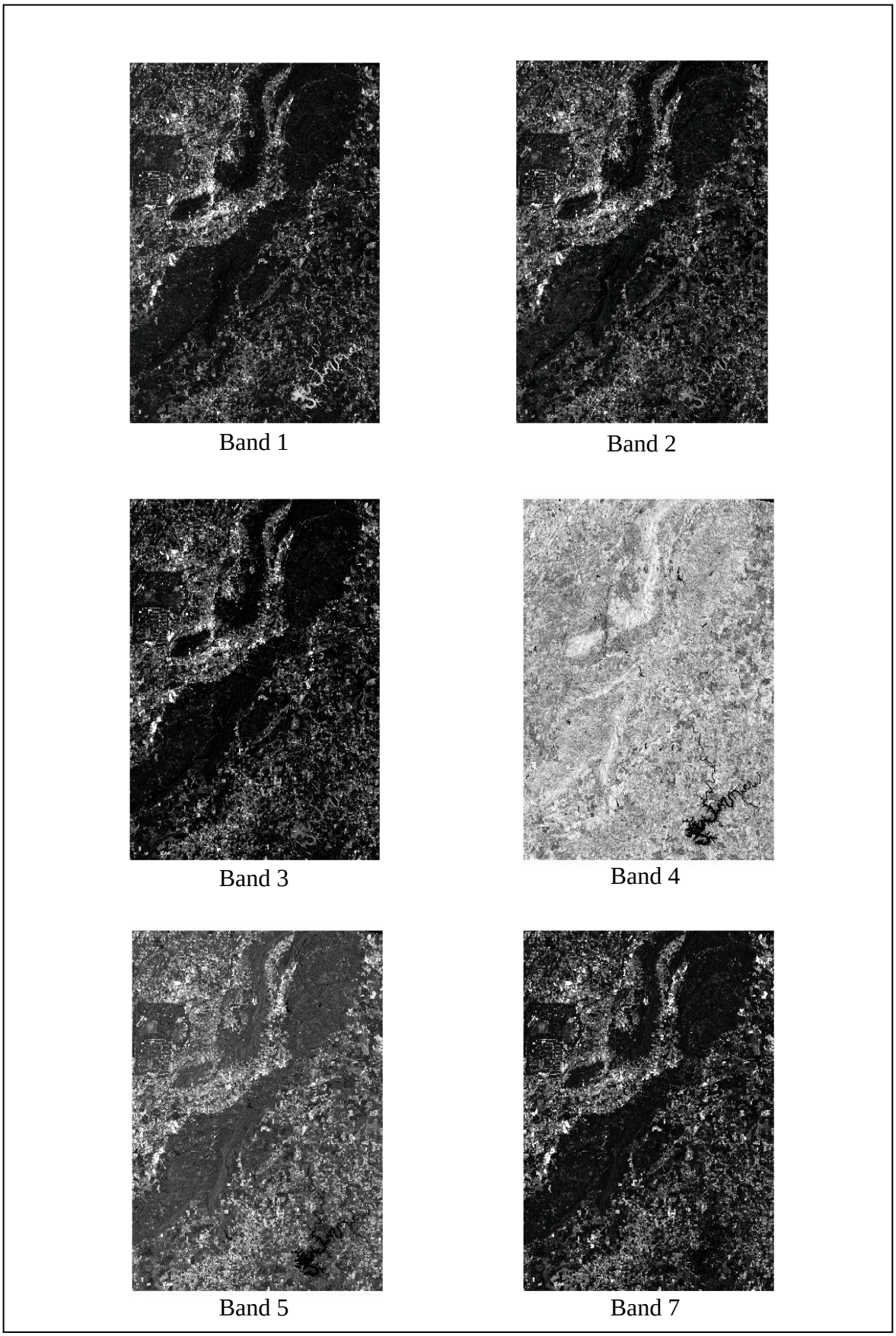

Figure 9. Multiple spectral images of Oakmulgee National Forest, AL, USA.

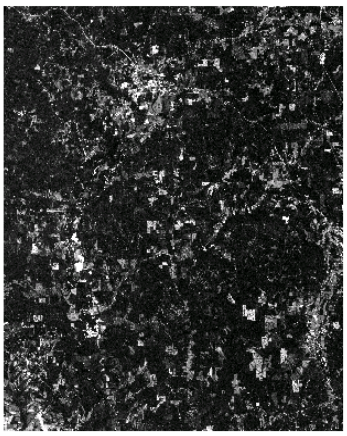

Band 1

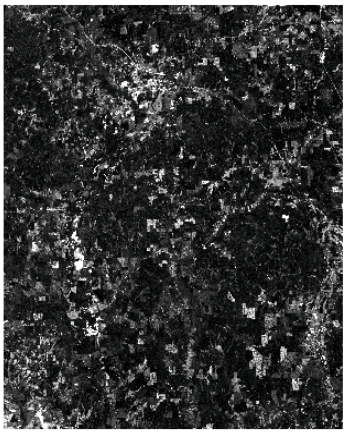

Band 2

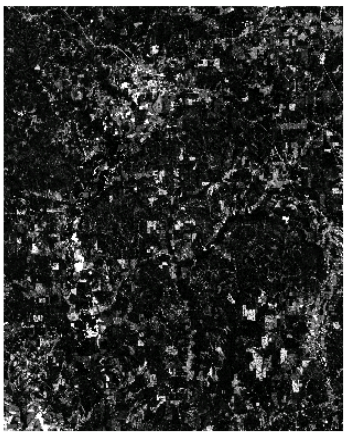

Band 3

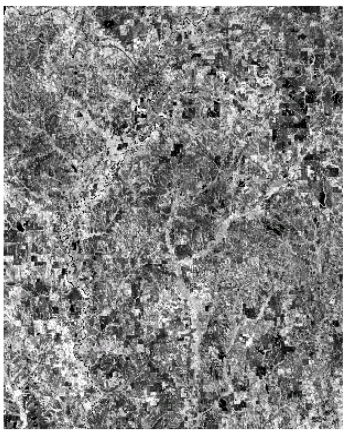

Band 4

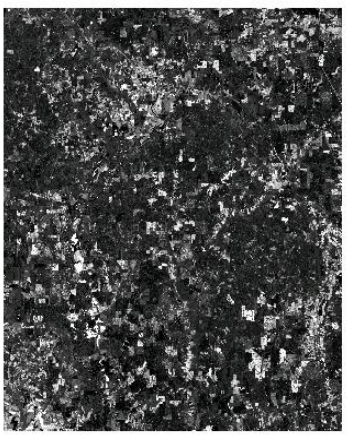

Band 5

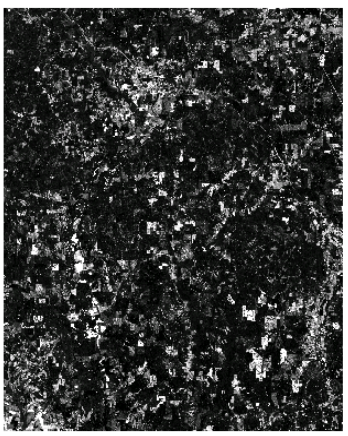

Band 7

Figure 10. Multiple spectral images of Bankhead National Forest, AL, USA.

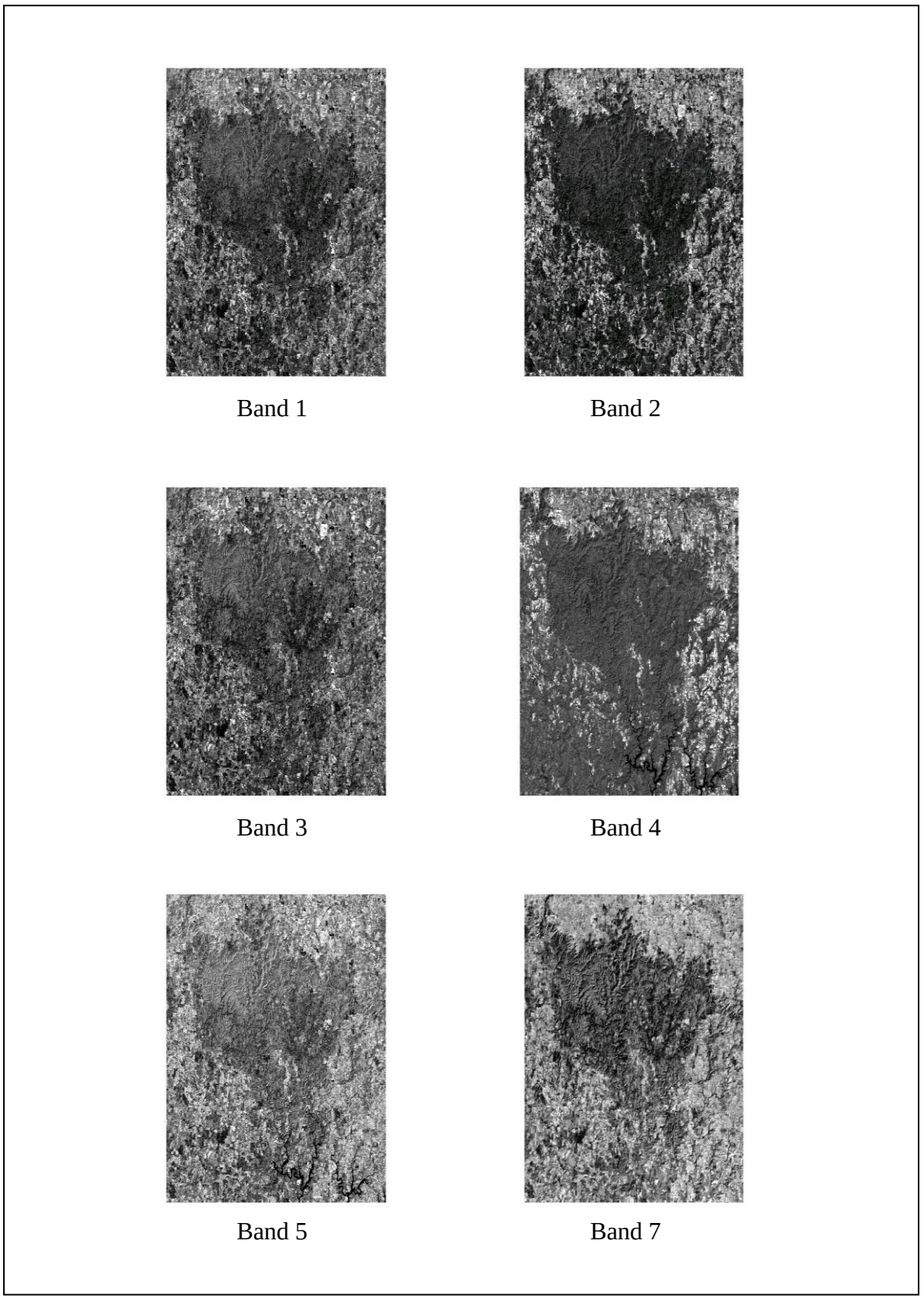

Figure 11. Multiple spectral images of Chatahoochee National Forest, GA, USA.

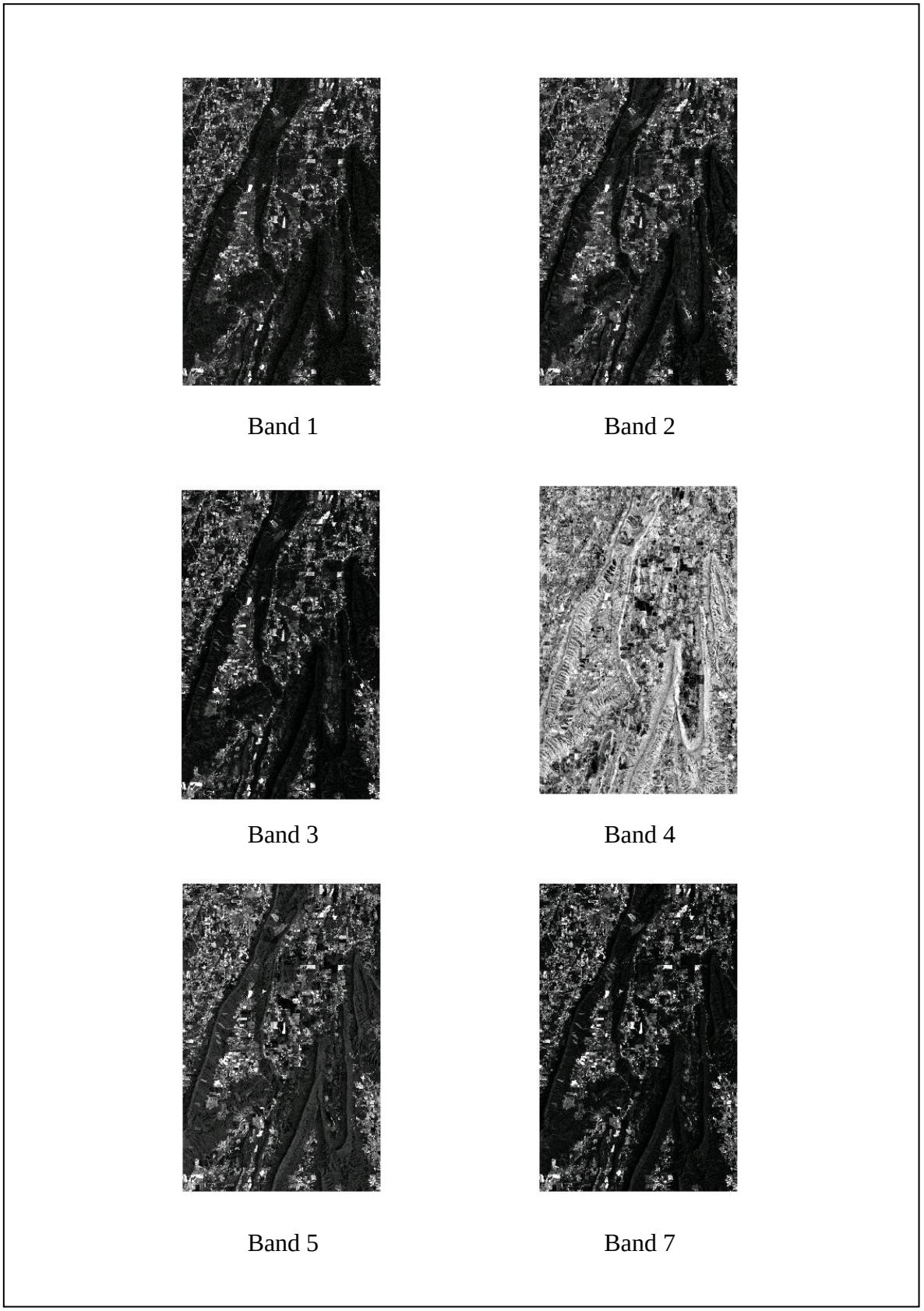

Figure 12. Fractal dimension values of samples within Talladega National Forest: **(a)** visible bands **(b)** near and middle infra red bands **(c)** all bands.

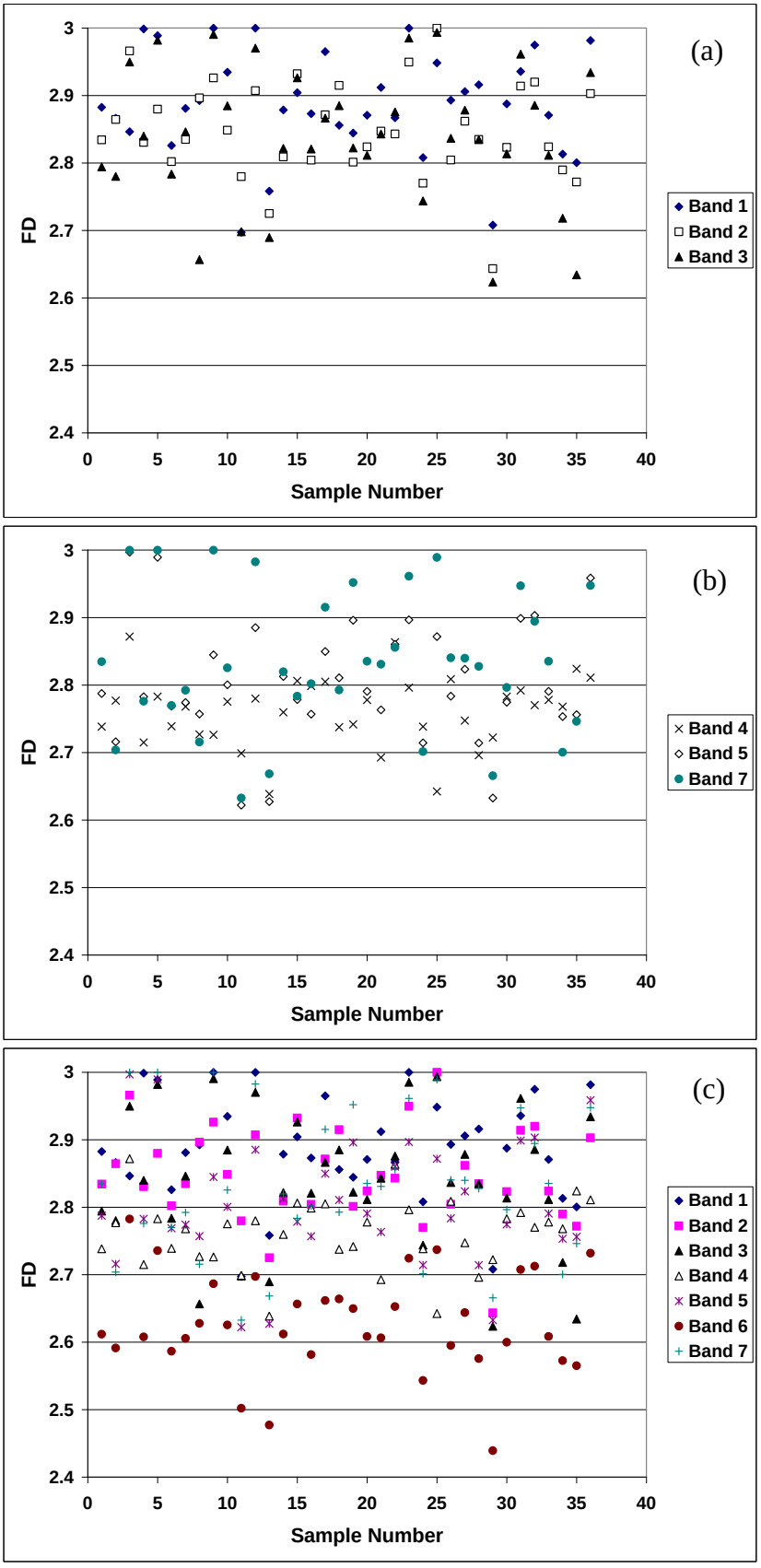

Figure 13. Fractal dimension values of samples within Oakmulgee National Forest: **(a)** visible bands **(b)** near and middle infra red bands **(c)** all bands.

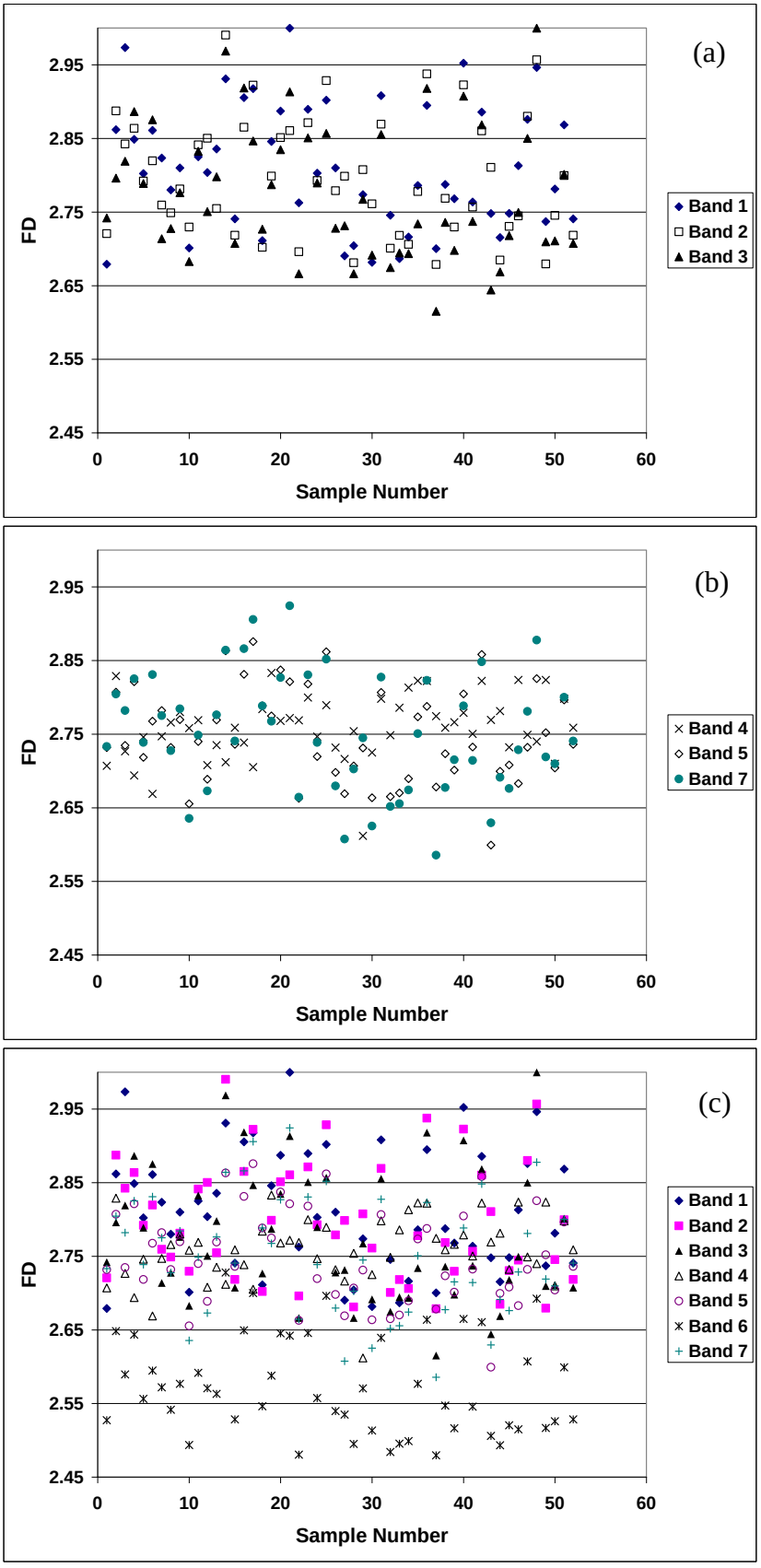

Figure 14. Fractal dimension values of samples within Bankhead National Forest: **(a)** visible bands **(b)** near and middle infra red bands **(c)** all bands.

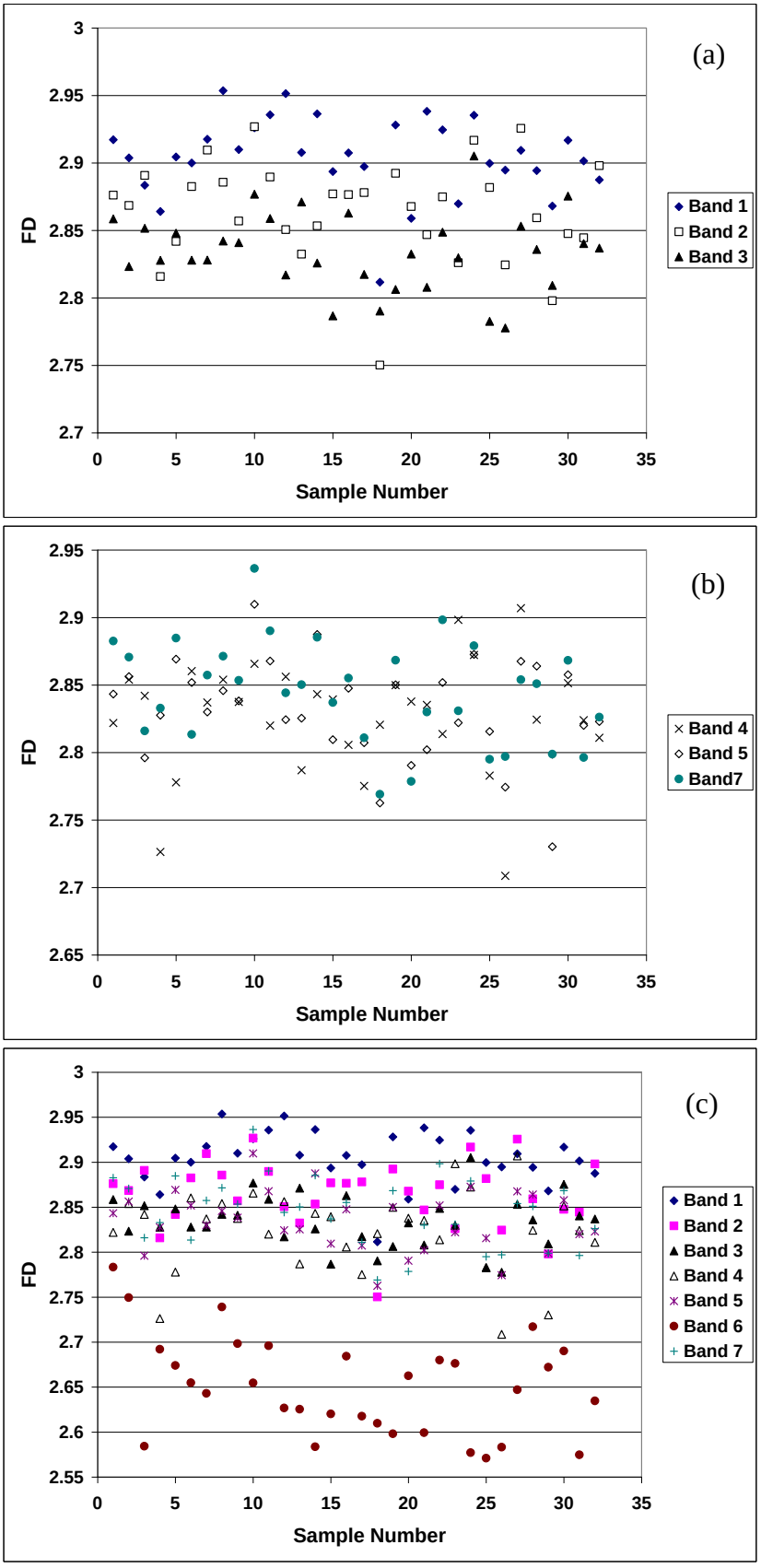

Figure 15. Fractal dimension values of samples within Chattahoochee National Forest: **(a)** visible bands **(b)** near and middle infra red bands **(c)** all bands.

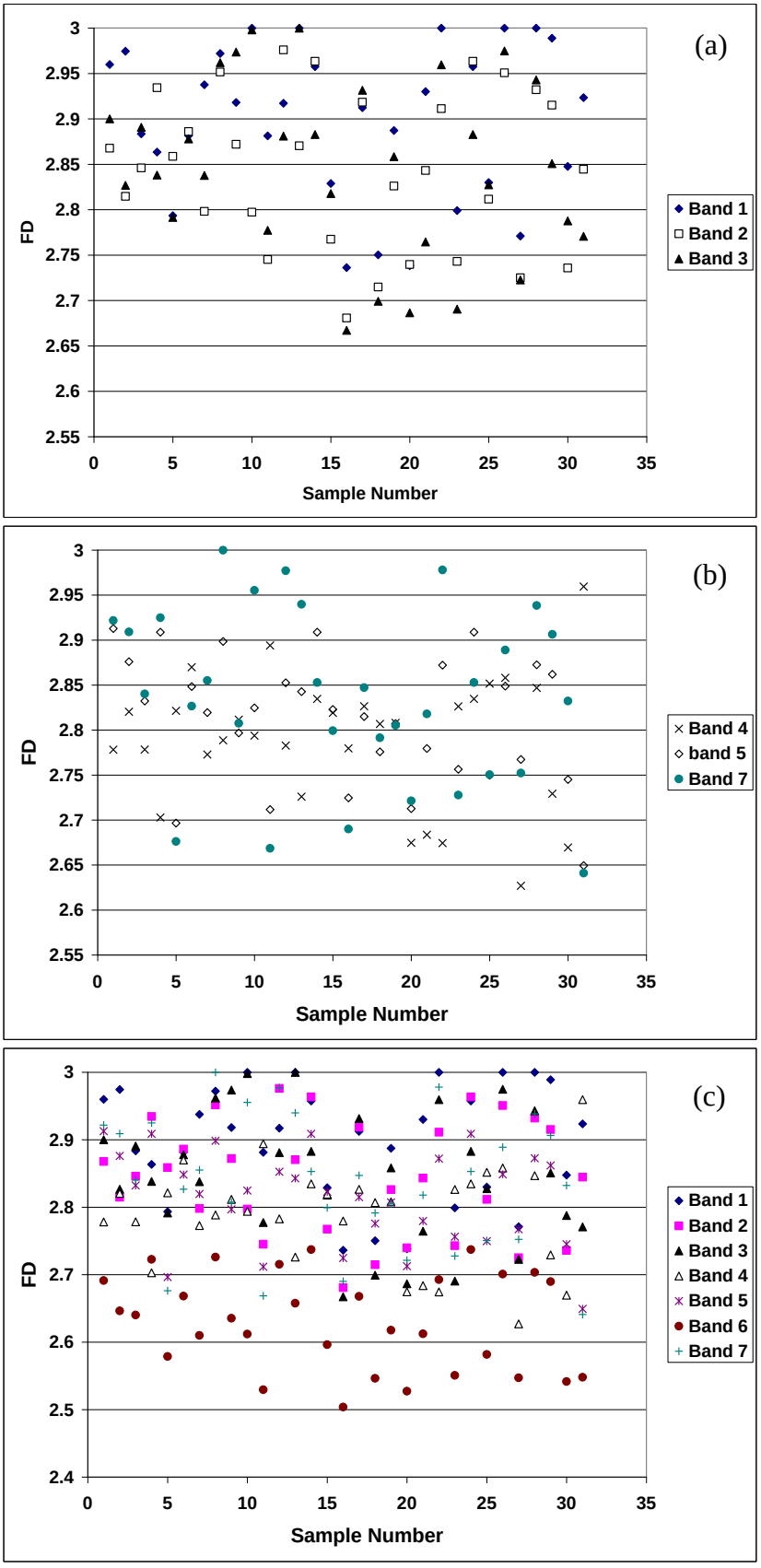

Table 5. Descriptive statistics of fractal dimensions for all bands: Talladega National Forest.

Statistic	**Fractal Dimension (FD)**						
	Band 1	Band 2	Band 3	Band 4	Band 5	Band 6	Band 7
Average	2.8885	2.8486	2.8386	2.7610	2.8040	2.6274	2.8328
Max	2.9999	2.9998	2.9935	2.8717	2.9968	2.7825	2.9999
Min	2.6973	2.6434	2.6235	2.6386	2.6220	2.4391	2.6327
Std. Dev.	0.0771	0.0706	0.1013	0.0513	0.0900	0.0746	0.1044
CV	0.0267	0.0248	0.0357	0.0186	0.0321	0.0284	0.0369

Table 6. Descriptive statistics of fractal dimensions for all bands: Oakmulgee National Forest.

Statistic	**Fractal Dimension (FD)**						
	Band 1	Band 2	Band 3	Band 4	Band 5	Band 6	Band 7
Average	2.8102	2.7960	2.7756	2.7591	2.7481	2.5731	2.7506
Max	2.9999	2.9904	2.9998	2.8331	2.8757	2.7279	2.9243
Min	2.6790	2.6787	2.6151	2.6118	2.5992	2.4795	2.5856
Std. Dev.	0.0840	0.0803	0.0886	0.0437	0.0638	0.0663	0.0796
CV	0.0299	0.0287	0.0319	0.0158	0.0232	0.0258	0.0289

Table 7. Descriptive statistics of fractal dimensions for all bands: Bankhead National Forest.

Statistic	**Fractal Dimension (FD)**						
	Band 1	Band 2	Band 3	Band 4	Band 5	Band 6	Band 7
Average	2.9046	2.8646	2.8343	2.8241	2.8347	2.6507	2.8448
Max	2.9536	2.9268	2.9052	2.9070	2.9098	2.7833	2.9364
Min	2.8116	2.7502	2.7777	2.7086	2.7626	2.5710	2.7691
Std. Dev.	0.0294	0.0374	0.0291	0.0453	0.0329	0.0546	0.0383
CV	0.0101	0.0130	0.0103	0.0160	0.0116	0.0206	0.0135

Table 8. Descriptive statistics of fractal dimensions for all bands: Chattahoochee National Forest.

Statistic	**Fractal Dimension (FD)**						
	Band 1	Band 2	Band 3	Band 4	Band 5	Band 6	Band 7
Average	2.8980	2.8453	2.8475	2.7887	2.8129	2.6301	2.8353
Max	2.9999	2.9759	2.9999	2.9594	2.9127	2.7371	2.9999
Min	2.7362	2.6807	2.6671	2.6270	2.6493	2.5037	2.6410
Std. Dev.	0.0839	0.0849	0.0959	0.0738	0.0705	0.0713	0.0982
CV	0.0289	0.0298	0.0337	0.0265	0.0251	0.0271	0.0346

4.1. Statistical Analysis

One-way ANOVA tests were conducted for the FD results of similar bands among all study areas (*i.e.*, Band 1 results from all study areas were compared to each other, Band 2 results from all study

areas were compared to each other, *etc*.). The ANOVA results showed that, at the 0.05 significance level, the FD values were significantly different in all visible bands. The p values for Band 1, Band 2, and Band 3 were 0.04, <0.001, and 0.01, respectively. The results also showed that, at the 0.05 significance level, the FD values were not significantly different for the infrared bands Band 5, Band 6, and Band 7. The p values for Band 5, Band 6, and Band 7 were 0.102, 0.232, and 0.273, respectively.

The results given above agree with the results of Quattrochi *et al.* [1] in which the authors found that as TM spectral band wavelength increases, Fractal Dimension values become more similar. These results also agree with the research done by Huang [49] who found that the variance of radiance over forest canopies with varying Leaf Area Index (LAI) were larger in the visible bands than in the mid and thermal infrared bands. Also, even for plants with similar LAI, reflectance in the visible wavebands with a higher chlorophyll content is lower than that of plants with a lower chlorophyll content. In contrast, reflectance in the near-mid infrared wavebands is almost identical [50]. So this suggests that the spectral responses from vegetation chlorophyll have a bigger influence on the Fractal Dimension (FD) (which is a measure of spatial heterogeneity) in the visible bands than would be the case in the near-mid infrared bands.

Figure 16 shows the average FD of the different bands for the four national forests. An examination of the average FD values from visible to middle-infrared bands for each study area indicates that the visible bands 1, 2, and 3 had the highest average FD values. The near and middle infrared bands 4 and 5 had the lowest average FD values. While the middle-infrared band 7 had average FD values that were in between. This could be attributed to the larger variance of radiance over forest canopies in the visible bands than in the near-mid infrared bands as explained previously rendering the images in those bands more heterogeneous or less homogonous. The more heterogeneous the remotely sensed image the more complex the surface will get in terms of fractals and the higher the fractal dimension will be. The thermal infrared (Band 6) has the lowest FD values among all bands for all study areas. As a matter of fact, FD values for Band 6 were very much lower than for all other bands. This dramatic drop in fractal dimension, and hence, image complexity, is believed to be due to the fact that TM Band 6 (*i.e.*, thermal infrared band 10.42–12.50 μm) is different from the other six TM bands because it has a spatial resolution of 120-m, while the other TM bands have a 30-m spatial resolution. Also, this thermal infrared band is an indicator of the surface temperature, which is relatively constant for trees, resulting in a homogonous surface and low FD. These trends in the average FD values among all Landsate TM spectral bands agree with the results of Zhao [44] that used fractals for the analysis of Landsat TM data to compare among different land cover types and forest was one of them. And they also agree with the results of Lam *et al.* [9] that have used fractals for the analysis of Landsat TM data for environmental assessment purposes.

An examination of the average fractal dimension (FD) values for each band indicates that the Bankhead National Forest image bands have the highest fractal dimensions among all the images, followed by Chattahoochee National Forest, Talladega National Forest, and Oakmulgee National Forest image bands. Additionally, a decrease in FD values is observed within the visible light wavelength region in all study areas, while an increase is observed in the near-infrared and middle-infrared regions. This corroborates the findings from previous studies [1,9,44] that have used fractals for the analysis of Landsat TM data.

Figure 16. Descriptive statistics of fractal dimensions for all bands: **(a)** average **(b)** standard deviation.

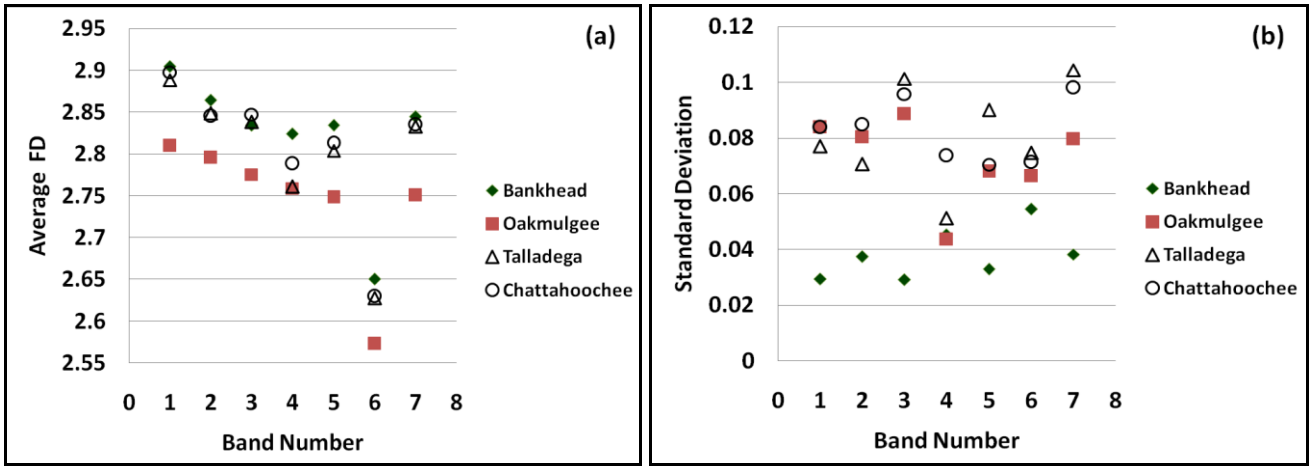

Finally, an examination of the average FD values for each band also indicates that the overall trend of the average FD values of all study areas (*i.e.*, national forests) is fairly constant throughout the entire spectral range (see Figure 16). However, the differences in FD values are noticeable among the four national forests except between Talladega National Forest and Chattahoochee National Forest which have the highest variation in elevation. That suggests that rough terrain could mask the effect of the differences in stand characteristics. Therefore, it appears that topographic factors are major contributors to spectral variation in high relief areas while the topographic effects are minimal and canopy characteristics are the primary determinants of spectral response in areas of gentle terrain. However, future research using more topographic parameters such as slope and slope aspect to evaluate the effect of topography on spectral variation and fractal dimensions in more detail is needed.

5. Summary and Conclusions

This study was aimed at determining the spatial resolution and spectral characteristics of remotely sensed instruments that would best characterize forested landscapes through the use of fractals. Initially, the effects of spatial resolution on the computed fractal dimensions were examined using data from three instruments with different spatial resolutions. Based on the criteria of mean value and variation within the accepted ranges of fractal dimensions, it was determined that 30-m Landsat TM data were best able to capture the complexity of a forested landscape in Central America compared to 4-m IKONOS data and 250-m MODIS data. This conclusion was based on the observation that the TM derived fractal dimensions were centered well within the desired range of 2.5–3.0 and that the sample values varied better within that range than did the fractals derived from the other data sets.

Next, among the spectral bands available on the TM, tests showed that the spatial indices of fractal dimensions are much more distinguishable in the Landsat TM visible bands than they are in the Landsat TM near-mid infrared bands. Thus, based solely on the fractal analysis, the fractal dimensions could have relatively higher chances to distinguish forest characteristics (e.g., stand sizes and species) in the Landsat TM visible wavelength bands than in the near-mid infrared bands. That could be attributed to the larger variance of radiance over forest canopies with varying Leaf Area Index (LAI) in the visible bands than in the near-mid infrared bands. Also, even for plants with similar LAI,

reflectance in the visible wavebands with a higher chlorophyll content is lower than that of plants with a lower chlorophyll content. In contrast, reflectance in the near-mid infrared wavebands is almost identical. Therefore, spectral responses from the vegetation chlorophyll have a bigger influence on the fractal dimension (which is a measure of spatial heterogeneity) in the visible bands than in the case of the near-mid infrared bands. This study has focused on a relative comparison between visible and near-mid infrared wavelength bands; however it will be important to study in the future the effect of a combination of those bands such as the Normalized Difference Vegetation Index (NDVI) on fractal dimensions of forested landscapes as well as the ability of fractal dimensions to help classify forest characteristics. Finally, additional work is also needed in order to confirm that the findings of this paper are generally evident in other forested landscapes with other species and canopy characteristics than those used in this study.

Acknowledgements

This project was supported by a grant from the U.S. Department of Transportation "Applications of remote sensing and related spatial technologies to environmental assessments in transportation." The assistance of the project manager, Roger King of Mississippi State University, and the USDOT program director, K. Thirumalai is gratefully acknowledged. The authors would also like to thank Nina Lam of Louisiana State University and Charles Emerson of Western Michigan University for their assistance.

References

1. Quattrochi, D.A.; Emerson, C.W.; Lam, N.S.-N.; Qiu, H.L. Fractal Characterization of Multitemporal Remote Sensing Data. In *Modeling Scale in Geographic Information Science*; Tate, N.J., Atkinson, P.M., Eds.; John Wiley & Sons, Ltd.: Hoboken, NJ, USA, 2001.
2. Goodchild, M.F.; Haining, M.; Wise, S. Integrating GIS and Spatial Data Analysis: Problems and Possibilities. *Int. J. Geogr. Inf. Syst.* **1992**, *6*, 407-423.
3. Mark, D.M.; Aronson, P.B. Scale-Dependent Fractal Dimensions of Topographic Surfaces: an Empirical Investigation, with Applications in Geomorphology and Computer Mapping. *Math. Geol.* **1984**, *11*, 671-684.
4. Lu, S.Z.; Hellawell, A. Using Fractal Analysis to Describe Irregular Microstructures. *J. Mater.* **1995**, *47*, 14-16.
5. Lovejoy, S.; Schertzer, D. Generalized Scale Invariance in Atmosphere and Fractal Models of Rain. *Water Resour. Res.* **1985**, *21*, 1233-1250.
6. Emerson, C.W.; Lam, N.S.-N.; Quattrochi, D.A. A Comparison of Local Variance, Fractal Dimension, and Moran's *I* as Aids to Multispectral Image Classification. *Int. J. Remote Sens.* **2005**, *26*, 1575-1588.
7. Lam, N.S-N.; Qiu, H.L.; Quattrochi, D.A.; Emerson, C.W. An Evaluation of Fractal Methods for Characterizing Image Complexity. *Cartogr. Geogr. Inf. Sci.* **2002**, *29*, 25-35.
8. Emerson, C.W.; Lam, N.S.-N.; Quattrochi, D.A. Multiscale Fractal Analysis of Image Texture and Pattern. *Photogramm. Eng. Remote Sens.* **1999**, *65*, 51-61.

9. Lam, N.S.-N.; Quattarochi, D.A.; Qiu, H.-L.; Zhao, W. Environmental Assessment and Monitoring with Image Characterization and Modeling System Using Multi-Scale Remote Sensing Data. *Appl. Geogr. Studies* **1998**, *2*, 77-93.
10. Mandelbort, B.B. *The Fractal Geometry of Nature*; W. H. Freeman: New York, NY, USA, 1983.
11. Goodchild, M.F. Fractals and the Accuracy of Geographical Measures. *Math. Geol.* **1980**, *12*, 85-98.
12. Shelberg, M.C.; Lam, N.S.-N.; Moellering, H. Measuring the Fractal Dimensions of Surfaces. In *Proceedings of the Sixth International Symposium on Automated Cartography (Auto-Carto 6)*, Ottawa, Canada, October 1983.
13. *Fractals in Geography*; Lam, N.S.-N., De Cola, L., Eds.; Prentice Hall: Englewood Cliffs, NJ, USA, 1993.
14. Lam, N.S.-N.; Qiu H.-L.; Quattrochi D. An Evaluation of Fractal Surface Measurement Methods Using ICAMS (Image Characterization and Modeling System). In *Proceedings of ACSM/ASPRS Annual Convention*, Seattle, WA, USA, April 1997.
15. Jaggi, S.; Quattrochi, D.A.; Lam, N.S-N. Implementation and Operation of Three Fractal Measurement Algorithms for Analysis of Remote Sensing Data. *Comput. Geosci.* **1993**, *19*, 745-767.
16. Krummel, J.R.; Gardner, R.H.; Sugihari, G.; O'Neill, R.V.; Coleman, P.R. Landscape Pattern in a Distributed Environment. *Oikos* **1987**, *48*, 321-324.
17. MacLennan, M.J.; Howarth, P.J. The Use of Fractal Geometry to Identify Ranges of Scale Variance in Digital Remotely Sensed Data. In *Proceedings of the 21st International Symposium on Remote Sensing Environment*, Ann Arbor, MI, USA, October 1987.
18. Palmer, M.W. Fractal Geometry: A Tool for Describing Spatial Patterns of Plant Communities. *Vegetatio* **1988**, *75*, 91-102.
19. Cohen, W.B.; Spies, T.A.; Bradshaw, G.A. Semivariograms of Digital Imagery for Analysis of Conifer Canopy Structure. *Remote Sens. Environ.* **1990**, *34*, 167-178.
20. Zeide, B. Fractal Geometry in Forestry Applications. *Forest Ecol. Manage.* **1991**, *46*, 179-188.
21. Lorimer, N.D.; Haight, R.G.; Leary, R.A. The Fractal Forest: Fractal Geometry and Applications in Forest Science. *General Technical Report NC-170*; US Department of Agriculture, Forest Service, North Central Forest Experiment Station, St. Paul, MN, USA, 1994.
22. St-Onge, B.A.; Cavayas, F. Automated Forest Structure Mapping from High Resolution Imagery Based on Directional Semivariogram Estimates. *Remote Sens. Environ.* **1997**, *61*, 82-95.
23. Barbanis, B.; Varvoglis, H.; Vozikis, C.L. Imperfect Fractal Repellers and Irregular Families of Periodic Orbits in A 3-D Model Potential. *Astron. Astrophys.* **1999**, *344*, 879-890.
24. Coops, N.; Culvenor, D. Utilizing Local Variance of Simulated High Spatial Resolution Imagery to Predict Spatial Pattern of Forest Stands. *Remote Sens. Environ.* **2000**, *71*, 248-260.
25. Weishampel, J.F.; Urban, D.L.; Shugart, H.H.; Smith, J.B. Semivariograms from a Forest Transect Gap Model Compared with Remotely Sensed Data. *J. Veg. Sci.* **1992**, *3*, 521-526.
26. Weishampel, J.F.; Sloan, J.H.; Boutet, J.C.; Godin, J.R. Mesoscale Changes in Textural Pattern of 'Intact' Peruvian Rainforests (1970s–1980s). *Int. J. Remote Sens.* **1998**, *19*, 1007-1014.
27. Weishampel, J.F.; Godin, J.R.; Henebry, G.M. Pantropical Dynamics of 'Intact' Rain Forest Canopy Texture. *Global Ecol. Biogeogr.* **2001**, *10*, 389-398.

28. Drake, J. B.; Weishampel, J.F. Simulating Vertical and Horizontal Multifractal Patterns of a Longleaf Pine Savanna. *Ecol. Model.* **2001**, *145*, 129-142.
29. Rocchini, D. Effects of Spatial and Spectral Resolution in Estimating Ecosystem α-Diversity by Satellite Imagery. *Remote Sens. Environ.* **2007**, *111*, 423-434.
30. Cao, C.; Lam, N.S.N. Understanding the Scale and Resolution Effects in Remote Sensing and GIS. In *Scale in Remote Sensing and GIS*; Quattrochi, D.A., Goodchild, M.F., Eds.; CRC/Lewis Publishers Inc.: Boca Raton, FL, USA, 1997.
31. Atkinson, P.M.; Curran, P.J. Defining an Optimal Size of Support for Remote Sensing Investigations. *IEEE Trans. Geosci. Remote Sens.* **1995**, *33*, 768-776.
32. Chen, D. Multi-resolution Image Analysis and Classification for Improving Urban Land Use/Cover Mapping Using High Resolution Imagery; Ph.D. Dissertation, San Diego State University and University of California: Santa Barbara, CA, USA, 2001.
33. Woodcock, C.E.; Strahler, A.H. The Factor of Scale in Remote Sensing. *Remote Sens. Environ.* **1987**, *21*, 311-332.
34. Marceau, D.J.; Howarth, P.J.; Gratton, R.A. Remote Sensing and the Measurement of Geographical Entities in a Forested Environment, 1. The Scale and Spatial Aggregation Problem. *Remote Sens. Environ.* **1994a**, *49*, 93-104.
35. Marceau, D.J.; Gratton, D.J.; Fournier, R.A.; Fortin, J.P. Remote Sensing and the Measurement of Geographical Entities in a Forested Environment, 2. The Optimal Spatial Resolution. *Remote Sens. Environ.* **1994b**, *49*, 105-117.
36. De Cola, L. Multiresolution Covariation among Landsat and AVHRR Vegetation Indices. In *Scale in Remote Sensing and GIS*; Quattrochi, D.A., Goodchild, M.F., Eds.; CRC/Lewis Publishers Inc.: Boca Raton, FL, USA, 1997.
37. Quattrochi, D.A.; Lam, N.S.N.; Qiu, H.L.; Zhao, W. Image Characterization and Modeling System (ICAMS): A Geographic Information System for the Characterization and Modeling of Multiscale Remote Sensing Data. In *Scale in Remote Sensing and GIS*; Quattrochi, D.A., Goodchild, M.F., Eds.; CRC/Lewis Publishers Inc.: Boca Raton, FL, USA, 1997.
38. Nellis, M.D., Briggs, J.M. The impact of Spatial Scale on Konza Landscape Classification Using Textural Analysis. *Landscape Ecol.* **1989**, *2*, 93-100.
39. Foody, G.M.; Curran, P.J. Estimation of Tropical Forest Extent and Regenerative Stage Using Remotely Sensed Data. *J. Biogeogr.* **1994**, *21*, 233-244.
40. Franklin, J.; Woodcock, C.E. Multiscale Vegetation Data for the Mountains of Southern California: Spatial and Categorical Resolution, In *Scale in Remote Sensing and GIS*; Quattrochi, D.A., Goodchild, M.F., Eds; CRC/Lewis Publishers Inc.: Boca Raton, FL, USA, 1980.
41. *Thirteen Ways of Looking at a Tropical Forest: Guatemala's Maya Biosphere Reserve*; Nations, J.D., Ed; Conservation International: Washington, DC, USA, 1999.
42. Clarke, K.C. Computation of the Fractal Dimension of Topographic Surfaces Using the Triangular Prism Surfaces Area Method. *Comput. Geosci.* **1986**, *12*, 713-22.
43. Myint, S.W. Wavelet Analysis and Classification of Urban Environment Using High-Resolution Multispectral Image Data; Ph.D. Dissertation, Louisiana State University: Baton Rouge, LA, USA, 2001.

44. Zhao, W. Multiscale Analysis for Characterization of Remotely Sensed Images; Ph.D. Dissertation, Louisiana State University: Baton Rouge, LA, USA, 2001.
45. Lefsky, M.A. Lidar Remote Sensing of Canopy Height Profiles: Application to Spatial and Temporal Trends in Canopy Structure; Ph.D. Dissertation, The University of Virginia: Charlottesville, VA, USA, 1997.
46. Watts, S.E. Determining Forest Productivity and Carbon Dyanamics in Southeastern Ohio from Remotely-Sensed Data; Ph.D. Dissertation, The Ohio State University, Columbus, OH, USA, 2001.
47. Bragg, D.C. A Local Basal Area Adjustment for Crown Width Prediction. *North. J. Appl. For.* **2001**, *18*, 22-28.
48. Walpole, R.E.; Myers, R.H. *Probability and Statistics for Engineers and Scientists*; Macmillan Publishing Company: New York, NY, USA, 1989.
49. Huang, J. Spatial Characterization and Analysis of Forests in the Mount Bachelor Volcanic Chain, Central Oregon; Ph.D. Dissertation, Oregon State University: Corvallis, OR, USA, 1998.
50. Zhang, R.H.; Sun, X.M.; Zhu, Z.L. A Remote Sensing Model for Determining Chlorophyll Content and its Distribution Using Landsat Images. *Acta Bot. Sin.* **1997**, *39*, 821-825.